

# a-Si/c-Si Heterojunction for Interdigitated Back Contact Solar Cell

Meijun Lu, Stuart Bowden, Ujjwal Das and Robert Birkmire  
Institute of Energy Conversion, University of Delaware, Newark, DE 19716

**Abstract:** Initial experimental and numerical simulation results for interdigitated back contact silicon heterojunction (IBC-SHJ) solar cell, which combines the high voltage potential of heterojunction solar cells while avoiding the absorption losses and allowing high short circuit currents, are reported. Cells without intrinsic buffer layers were fabricated as a proof of concept. The cells with intrinsic buffer layer show open circuit voltage of 683 mV, but with low fill factors, and optimization to reduce this effect is undergoing. Two-dimensional theoretical simulation through software package Sentaurus Device is applied to model the device, where distribution of trap states and thermionic emission were considered for a-Si:H material and a-Si:H/c-Si hetero-interface, respectively. The model results can be correlated to both J-V measurements and LBIC scans. Both experiments and simulation show that the performance of IBC-SHJ solar cell depends on the front surface recombination velocity. Also the model demonstrates that the IBC-SHJ solar cells allow efficiencies in excess of 22%.

## 1. Introduction

The rapid market growth of silicon (Si) solar cells is driving the development of devices using thinner Si wafers and higher efficiency technologies [1]. An interdigitated back contact silicon heterojunction (IBC-SHJ) solar cell [2], which combines the advantages of both IBC [3] and SHJ [4] techniques, is an attractive device structure for achieving this. IBC-SHJ combines the high voltage potential of heterojunction solar cells while avoiding the absorption losses in these structures and allowing the high short circuit currents of a rear junction back contact solar cell. It also has the advantage of entirely low temperature processing sequence [2]. In this work, initial experimental results for IBC-SHJ cells without and with intrinsic buffer layers are shown. Software package Sentaurus Device is applied to get two-dimensional modeling of IBC-SHJ solar cell. Also the dependence of IBC-SHJ cells to the front surface passivation is discussed both experimentally and theoretically through numerical simulation.

## 2. Experiments and initial cell results

The schematic of the IBC-SHJ solar cell is shown in Figure 1. The cells were fabricated on 300  $\mu\text{m}$  thick, polished, n-type float-zone silicon wafer with resistivity of 2.5  $\Omega\text{cm}$ . All a-Si:H layers, intrinsic, p-type and n-type, were deposited in a multi-chamber direct current (DC) plasma enhanced chemical vapor deposition (PECVD) system at 200°C. The front surface was passivated with a 20 nm intrinsic a-Si:H layer followed by AR coatings composed of Indium Tin Oxide (ITO) and  $\text{MgF}_2$ , deposited by sputtering and electron beam evaporation respectively. This surface passivation/antireflection structure is not ideal for high  $J_{\text{SC}}$  but provided a means of evaluating the device performance and the utility of the structure as a diagnostic tool to evaluate surface recombination. At the back of the wafer, the emitter and contacts consist of interdigitated p- and n-type a-Si:H layers respectively at a thickness of 20 nm. A 200 nm thick aluminum deposited by electron beam evaporation is used as a robust contact

for testing. For the case of with back surface intrinsic buffer layer, an 8 nm intrinsic a-Si:H was added to the whole back surface before the deposition of p-/n- type a-Si:H layers. The interdigitated pattern was created by two-step photolithography processing where the p-region has lateral dimension of 1.2 mm and n-region is 0.5 mm wide. The numbers of p-strip and n-strip are fixed at 5 and 4 respectively with a cell area of 1.37 cm<sup>2</sup>. The separation between p- and n-regions is ~2 μm for the cell without rear intrinsic buffer layer, which is formed naturally by undercutting during the etching process. While in the cell with rear intrinsic buffer layer, a separation of ~50 μm was achieved through masking during photolithography, since the etching process should be avoided to keep the passivation effect of the back surface intrinsic buffer layer.

Figure 2 shows the initial results of J-V curve under AM1.5 illuminations, where the solid curve is the sample without intrinsic buffer layer, and the dashed curve is the one with i-

layer. It can be seen that for the case without i-layer, fill factor (FF) is high (74%) and there is no evidence of shunting between the p- and n-type regions, which demonstrates the robust nature of the process and proves the concept of the structure. For the case of with passivating i-layer, a higher V<sub>OC</sub> of 683 mV and a larger J<sub>SC</sub> of 36 mA were obtained, while the FF is low and the JV curve shows “S-shape”. This S-shape JV curve has also been observed in the front junction cell [5] and was resolved through process optimization. Optimizations to reduce this effect in IBC-SHJ solar cell are undergoing.

### 3. 2D Modeling with Sentaurus Device

To better understand the performance of IBC-SHJ solar cell, numerical simulation of the device is studied through Synopsys device modeling package Sentaurus Device (version Y-2006.06). The structure of IBC-SHJ solar cell used in simulation is similar to Fig.1 except that the front surface AR coatings and the buffer i-layer are replaced by a single passivation layer of SiN<sub>x</sub> (70nm). This ideal front surface simplifies the cell structure and it can still simulate the device performance very well with only a little difference in current due to the different anti-reflection effect.

The three governing semiconductor equations, Poisson equations and the electron and hole continuity equations, together with drift-diffusion model [6] in Sentaurus Device were used, and the impurity scattering and carrier-carrier scattering were considered. The Auger and Shockley-Read-Hall recombination were modeled as a function of doping concentration. For the a-Si layers, the critical parameters are the energy distribution of

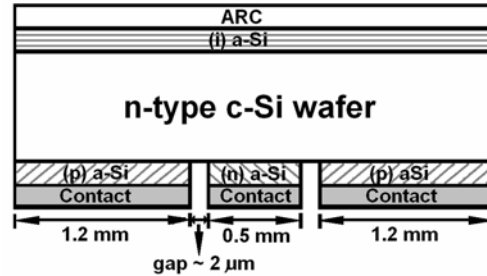


Figure 1. Schematic picture of the IBC-SHJ structure, where two p-strips and one n-strip are shown. For clarity, the cell thickness is greatly exaggerated.

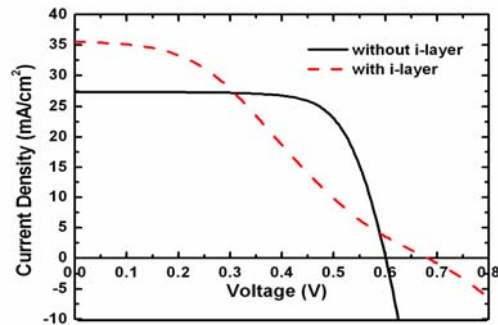


Figure 2. Illuminated (AM1.5) J-V for IBC-SHJ cells, without (solid curve) and with (dashed curve) back surface buffer i-layer.

the exponential band tails, and the Gaussian distribution of the mid-gap trap states. They were chosen based on Reference [7] and were tuned to fit the properties, dark and light conductivity, of deposited a-Si layers. For c-Si/a-Si interfaces at the back surface, a thermionic emission model was used, in which the distribution function of the interface defect is modeled by two capture cross-sections, one for the holes and one for the electrons. An AM1.5G solar spectrum is used for the optical generation to simulate the current density-voltage (J-V) curve under standard one-sun illumination conditions at an intensity of  $100 \text{ mW/cm}^2$ .

#### 4. Effect of front surface passivation

It was noticed that the performance of IBC-SHJ solar cell depends on how the front surface is passivated [2]. Figure 3 shows the reflection corrected internal quantum efficiency (IQE) for the same IBC-SHJ cell characterized at three stages in the process sequence: before anti-reflection coating (ARC), after ARC, and after annealing with ARC. The cell's performance decreases after application of the ARC, but improves after annealing to exceed the initial device performance. The modeling software PC1D was used to fit the IQE curves (dashed lines), and extract the front surface recombination velocity. It turns out that the front surface recombination velocity,  $S$ , increases from  $152 \text{ cm/s}$  to  $299 \text{ cm/s}$  after ARC, while decreasing to  $82 \text{ cm/s}$  after annealing. This change of front surface recombination causes the different cell performance.

Simulation of IBC-SHJ solar cell with different front surface recombination velocity ( $S$ ) at  $\text{SiN}_x/\text{c-Si}$  interface was performed and the resulting J-V curves are shown in Figure 4. As seen, both  $J_{SC}$  and  $V_{OC}$  increase as  $S$  decreases, resulting in higher cell efficiency. Since most carriers are generated near the front surface, while the p-n junction is far at back surface, high front  $S$  would cause carrier recombination before they reach the back junction. Hence front surface passivation is especially important for IBC-SHJ solar cell. With low front  $S$  of  $10 \text{ cm/s}$ , a value that is achievable and consistent with lifetime measurements of  $2.2 \text{ milliseconds}$ , the 2D modeling shows that IBC-SHJ cell can attain an efficiency of  $22\%$  when back surface is well passivated.

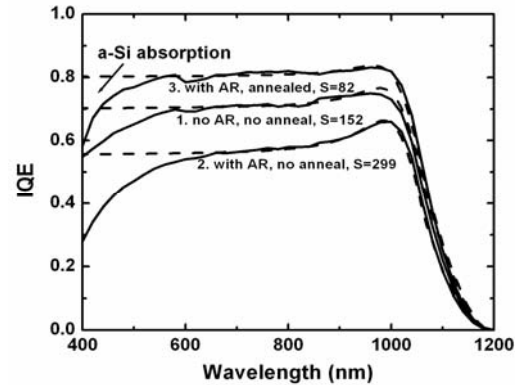


Figure 3. Same sample at three stages show the IBC-SHJ cell performance depends on the front surface recombination velocity ( $S$ ).

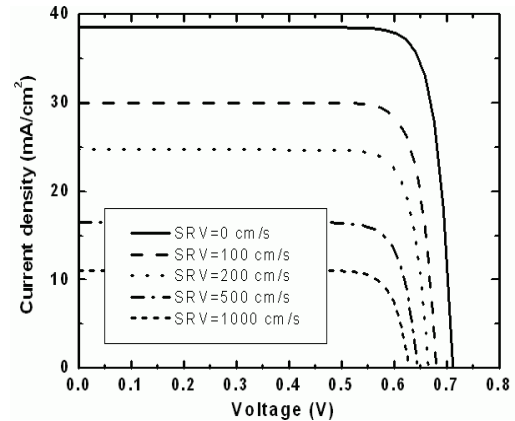


Figure 4. Simulated J-V curve for IBC-SHJ cell with different front surface recombination velocity ( $S$ ).

To further investigate the device performance, the cell with  $S=80$  in Fig.3 was measured using light beam induced current (LBIC) and compared to the theoretical calculations, where the LBIC line scan was simulated using a  $50\mu\text{m}$  wide white light beam scanning from left to right on the device. The simulation matches the experimental results well and they are shown in Figure 5. It can be seen that p-region has higher current than n-region, this is because that carriers generated at the p-type strips with the collection junction are more likely to be collected than carriers above the n-type strips, which have to diffuse laterally to a p-type strip. The high degree of correlation between the LBIC measurement and the Sentaurus model further confirms the validity of the determination of the front surface recombination velocity at  $80\text{ cm/s}$  in Fig.3.

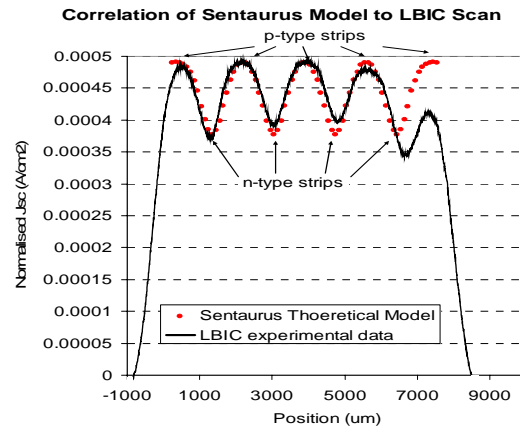


Figure 5. Comparison of theoretical model and experimental data for a LBIC scan.

## 5. Conclusions

Initial experimental and numerical simulation results for interdigitated back contact silicon heterojunction (IBC-SHJ) solar cell were presented. IBC-SHJ solar cells without intrinsic buffer layers proved robust nature of the structure. The cells with intrinsic buffer layer have shown  $V_{OC}$  of  $683\text{ mV}$  and  $J_{SC}$   $36\text{ mA}$ , but with low FFs, and optimization to reduce this effect is undergoing. 2D modeling through Sentaurus Device is applied to simulate the device. Both experiments and modeling show that the front surface passivation is very important for IBC-SHJ solar cell. LBIC line scan was simulated and matched with experimental result well. The simulations suggest that by reducing front SRV to  $10\text{ cm/s}$ , efficiency of  $22\%$  can be achieved for IBC-SHJ solar cell.

## Acknowledgment

This work was partly supported by National Renewable Energy Laboratory under subcontract #ADJ-1-30630-12.

## References:

- [1] S.W.Glunz, *Sol.Energ.Mat.Sol.C*, **90**, 2006, pp.3276-3284.
- [2] M.Lu, S.Bowden, U.Das, M.Burrows and R.Birkmire, *Appl.Phys.Lett.*, In press.
- [3] M.D. Lammert and R.J. Schwartz, *IEEE T. Electron Dev.*, **24** (4), 1977, pp.337.
- [4] M. Taguchi, K. Kawamoto, S. Tsuge, T.Baba, H.Sakata et al., *Prog. Photovoltaics* **8** (5), 2000, pp.503.
- [5] U. Das, S. Bowden, M. Burrows, S. Hegedus and R.Birkmire, *4th World Conference on Photovoltaic Energy Conversion*, Hawaii, USA, 1283 (2006).
- [6] Manual for Sentaurus Device from Synopsys Inc., Version Y-2006.06.
- [7] R.E.I.Schropp, M.Zeeman, *Amorphous and micro-crystalline silicon solar cells*, Kluwer Academic, Dordrecht, 1998, pp.183.